Phosphorylated cellulose propionate derivatives as thermoplastic flame resistant/retardant materials: influence of regioselective phosphorylation on their thermal degradation behaviour

Dan Aoki · Yoshiyuki Nishio*

Division of Forest and Biomaterials Science, Graduate School of Agriculture, Kyoto University, Sakyo-ku, Kyoto 606-8502, Japan

* To whom correspondence should be addressed. E-mail: ynishio@kais.kyoto-u.ac.jp. Tel.: +81 75 753 6250. Fax: +81 75 753 6300.

Abstract Cellulose ester derivatives having phosphoryl side-chains were synthesized by phosphorylation of two types of cellulose propionate (CP); the difference between the two CPs was whether the primary hydroxyl group at C6 had been fully propionylated or not. Dimethyl phosphate, dimethyl thiophosphate, diethyl phosphate, or diethyl thiophosphate was introduced into the residual hydroxyl positions of the CPs. Chemical composition of the respective derivatives was characterized by elemental analysis and a combined use of saponification and HPLC quantification of the released propionic acid. Their thermal properties were investigated by DSC and TGA, and an intermediate residue of the pyrolysis was also examined by FT-IR spectroscopy. From the thermal degradation measurements using TGA, the C6-*O* phosphorylation was found to noticeably prevent the CP derivatives from weight loss in the pyrolysis process under dynamic air, i.e., providing them with a flame-resistance functionality, whereas the C2-*O* and C3-*O* phosphorylation did not give rise to such an appreciable resistance effect. A discussion was focused on the difference in pyrolysis mechanism between the phosphorylated CPs. However, most samples of the CP derivatives showed a clear T_g considerably lower than the onset temperature of the thermal degradation. Thus we suggest that it is possible to design thermoplastic flame resistant/retardant materials based on cellulose, by controlling the substitution distribution of the phosphoryl and propionyl groups introduced.

Keywords Cellulose propionate · Phosphorylation · Flame resistance · Regioselective functionalization

Introduction

Flammability seems to be a weak point of cellulosic materials. In the past, a number of researches have been conducted on fabrication of flame-resistant cellulosic fibers or design of flame-retardants for fibrous celluloses (e.g. Kandola et al. 1996; Price et al. 1997). The employment of phosphoric acids or phosphates as a dispersing retardant may be a promising approach to obtain flame-resistant cellulosic materials. The flame retardability of phosphoric acids for cellulose is ascribable to dehydrating the polysaccharide molecules and promoting the consequent char formation. In the process, the phosphoric acid used acts as an acid catalyst; particularly, an interaction between the phosphoric acid and C6 hydroxyl group is considered to be important for protecting the generation of levoglucosan accompanying cleavage of $\beta(1\rightarrow4)$ glycosidic linkage (Pacsu and Schwenker 1957). This interaction involves a route of esterification of the phosphoric acid at the hydroxyl group (Kandola and Horrocks 1996), and, therefore, a phosphoryl derivatization (phosphorylation) of cellulose should also be effective for the flame retardation. Furthermore, in comparison with external flame-retardant additives, there is another advantage for the 'internal' phosphorylation, i.e., it causes no bleeding-out problem.

Chemical modification of the hydroxyl groups of cellulose at C2, C3, and C6 positions is the most common way to furnish new functionalities to cellulosic materials (Klemm et al. 2005; Nishio 2006; El Seoud and Heinze 2005). Recent studies of cellulose functionalization involve a regioselective modification for optimization of the desired functionality (Karakawa et al. 2007; Klemm et al. 2005). As regards the improvement in flame resistance of cellulosics with phosphoric acid, little attention has been paid to the contribution of a possible interaction between the phosphoric acid and C2/C3 OH to the flame-retarding effect, even though the interaction with C6 OH might be substantial as

mentioned above.

The main purpose of the present study is to prepare phosphorylated cellulose derivatives and investigate the flame-resistant behaviour with attention to some influence of the phosphorylation position. If the derivatization is carried out by regioselective functionalization, e.g., via substitutions of a phosphoryl group and another one at the respectively preferential positions, the investigation will provide a hint for designing a novel cellulosic flame-retarding material of thermoplasticity. In this paper, we synthesized cellulose ester derivatives having phosphoryl side-chains by phosphorylation of two types of cellulose propionate (CP); the difference between the two CPs was whether the primary hydroxyl group at C6 had been fully propionylated or not. The propionyl moiety should also serve a thermoplasticity to the final products. Thermal transitions and degradation of the phosphorylated CP derivatives are investigated by differential scanning calorimetry (DSC) and thermogravimetric analysis (TGA). Moreover, an attempt is made to infer a flame-retarding mechanism for the derivatives through analysis of FT-IR spectra of intermediate residues of the pyrolysis.

Experimental

Materials

Microcrystalline cellulose Avicel® (hereafter Avicel) was purchased from Merck KGaA and used as received. Two types of cellulose propionate (CP1 and CP2) were used. CP1 was synthesized from Avicel and the detailed procedure will be described below. CP2 was purchased from Scientific Polymer Products, Inc. and purified before use to remove a

plasticizer (dioctyl adipate) by dissolving in acetone, reprecipitating into distilled water, and washing with ethanol. *N*,*N*-Dimethylacetamide (DMAc; Nacalai Tesque, Inc.), *N*,*N*-dimethylformamide (DMF; Nacalai Tesque, Inc.), pyridine (Py; Nacalai Tesque, Inc.), and triethylamine (Wako Pure Chemical Industries, Ltd.) were stored over molecular sieves 4A for 3 days before use. Lithium chloride (LiCl) was purchased from Nacalai Tesque, Inc. and dried at 140 °C for 4 h in a vacuum oven. Diethyl chlorophosphate, diethyl chlorothiophosphate, dimethyl chlorophosphate, and dimethyl chlorothiophosphate were purchased from Sigma-Aldrich, Inc. and used as received. Propionyl chloride, acetic anhydride, 4-(dimethylamino)pyridine, chloroform ($CHCl_3$), propionic acid, dimethylsulfoxide (DMSO), tetrahydrofuran (THF), and other reagents were purchased from Wako Pure Chemical Industries, Ltd. and used as received. Nitrogen gas (99.95 %) and air gas (synthetic air ZERO-A: O_2 = 20–21.5 %; CO < 1 ppm; CO_2 < 2 ppm; H_2O < 10 ppm) were purchased from Sumitomo Seika Chemicals Co., Ltd.

Synthesis of cellulose propionate (CP1)

A cellulose solution in DMAc-LiCl was prepared in almost the same way as that adopted in a previous study (Nishio et al. 1987). The salt content in the solvent system DMAc-LiCl was 7 wt %. The cellulose powder Avicel treated by a solvent-exchange technique successively with distilled water, ethanol, and DMAc was added to DMAc-LiCl, and the mixture was stirred at room temperature until dissolution of the cellulose was completed. The actual concentration of cellulose in the solution was adjusted to 4.0 wt %.

Cellulose propionate (CP1) was synthesized with acid chloride/base catalyst from the above-mentioned cellulose solution in a way similar to that used in a previous study (Nishio et al. 1997). A solution of 17.8-mL triethylamine (2 eq/anhydroglucopyranose unit (AGU))

in 17.8-mL DMAc was slowly added dropwise to a 250-g portion of the Avicel solution. After 20 min, a solution of 21.5-mL propionyl chloride (4 eq/AGU) in 21.5-mL DMAc was added to the cellulose solution. The reactive solution system was stirred continuously at 40 °C under a nitrogen atmosphere. After 16 h, the solution was reprecipitated in an excess amount of distilled water. The product was purified by dissolving in acetone and reprecipitating into distilled water, followed by drying at 40 °C for 48 h in a vacuum oven.

Acetylation of CP1 and CP2

To obtain well-resolved NMR spectra required for determining the substitution distribution of propionyl side-chains, CPs were acetylated. 0.1-g CP and 0.05-g 4-(dimethylamino)pyridine were added to 10-mL Py, and the mixture was stirred for 10 min at 20 °C. The resulting solution was heated to 40 °C and 1.5-mL acetic anhydride was dropped thereinto. After 4 h, the solution was reprecipitated in an excess amount of distilled water. The acetylated CP was purified by dissolving in acetone and reprecipitating into distilled water, and then dried at 40 °C for 48 h in a vacuum oven. Completion of the acetylation was confirmed by FT-IR measurements; a band centering ~3500 cm^{-1}, derived from OH stretching vibration, vanished after the acetylation.

Synthesis of phosphorylated CP derivatives

Diethylphosphorylated CP (DEP-CP), diethylthiophosphorylated CP (DETP-CP), and dimethylphosphorylated CP (DMP-CP) were synthesized as follows. 1.0-g Cellulose propionate (CP1 or CP2) was dissolved in 20-g Py. The mixture was heated at 40 °C, and diethyl chlorophosphate, diethyl chlorothiophosphate, or dimethyl chlorophosphate (8

eq/AGU) diluted with an equivalent quantity (ca. 4.0–5.2-g) of chloroform was dropped thereinto. The reactive solution system was stirred continuously at 40 °C under a nitrogen atmosphere. After 24 h, the solution was reprecipitated in an excess amount of distilled water. The crude product obtained as precipitate was purified by dissolving in acetone and reprecipitating into distilled water. The purified sample was freeze-dried for 1 week.

Dimethylthiophosphorylated CP (DMTP-CP) was synthesized as follows. 1.0-g cellulose propionate (CP1 or CP2) was dissolved in a mixture of ca. 3.2-g Py (12 eq/AGU) and 20-g chloroform. The resulting solution was then heated at 40 °C and dimethyl chlorothiophosphate (8 eq/AGU) diluted with 4.4-g chloroform was dropped thereinto. The reaction system was stirred continuously at 40 °C under a nitrogen atmosphere and reflux. After 30 h, the solution was reprecipitated in an excess amount of 2-propanol. The product obtained as precipitate was purified in a procedure similar to that stated above.

Basic hydrolysis of CP and phosphorylated CP derivatives

0.1-g Powder of CP or phosphorylated CP derivatives was suspended and stirred in 15-mL 2 M NaOH aq at 70 °C. After 24 h, the mixture was cooled to 25 °C and 30-mL 1M HCl aq was added thereinto. After stirring for 2 h at 25 °C, the mixture was filtered and the filtrate was diluted to 100 mL with distilled water in a volumetric flask. The diluted filtrate was used for high-performance liquid chromatography (HPLC) measurements to evaluate the propionic acid content (see below). The hydrolyzed residue filtered off was washed with ethanol and then dried at 40 °C for 48 h in a vacuum oven. Completion of the basic hydrolysis of propionyl groups for CP was confirmed by FT-IR measurements; a band centering ~1750 cm^{-1}, derived from C=O stretching vibration, vanished after the hydrolysis.

Measurements

300-MHz ^{1}H NMR and 75-MHz quantitative ^{13}C NMR spectra were measured by using a Varian INOVA 300 NMR apparatus. The measuring conditions of ^{1}H NMR were as follows: solvent, $CDCl_3$; solute concentration, 30 mg mL^{-1}; internal standard, tetramethylsilane (TMS); temperature, 20 °C; number of scan, 64; recycle time, 6.5 s. The quantitative ^{13}C NMR measurements were performed by an inverse-gated decoupling technique in the following conditions: solvent, $CDCl_3$; solute concentration, 30 mg mL^{-1}; internal standard, TMS; temperature, 20 °C; number of scan, 4096; recycle time, 50 s.

Gel permeation chromatography (GPC) was carried out with a Tosoh HLC-8220 GPC apparatus. The measuring conditions were as follows: column, two Tosoh TSK Super HZM-H columns connected with each other; flow rate, 0.25 mL min^{-1}; temperature, 40 °C; eluent, THF; standard, monodispersed polystyrene.

Elemental analysis was carried out with a Yanaco CHN Corder MT series (for C and H quantifications) and a Shimadzu UV-1700 Phamaspec (for P quantification). All the measurements were duplicated for each sample of phosphorylated CP, and the respective carbon (C) and phosphorous (P) contents were evaluated with a tolerance of <1.5 %.

HPLC measurements were made by using a Shimazu RID-7 apparatus to determine the content of propionyl side-chains for CP1, CP2, and phosphorylated derivatives from the CPs. The measuring conditions were as follows: column, a STR ODS-II (Shinwa Chemical Industries, LTD.); flow rate, 0.6 mL min^{-1}; temperature, 40 °C; eluent, 0.024 wt % perchloric acid aqueous solution.

DSC analysis was carried out with a Seiko DSC6200/EXSTAR6000 apparatus. The temperature proof-readings were calibrated with an indium standard. For a given polymer

sample, two thermograms were collected with a set of two aluminum pans each containing ca. 4-mg of the sample, under a nitrogen atmosphere. One sample pan was solely heated from ambient temperature (25 °C) to 280 °C at a scanning rate of 20 °C min^{-1} (first heating scan). Next, the other pan was heated from 25 to 160–180 °C and then immediately cooled to −50 °C at a rate of 80 °C min^{-1}. Following this, a heating thermogram was monitored at 20 °C min^{-1} over the temperature range of −50–250 °C (second heating scan). A starting temperature of polymer degradation, $T_{d\text{-}DSC}$, was estimated in the first heating scan and taken as a temperature at the onset of an abrupt exothermic ascent. The glass transition temperature T_g was determined in the second heating scan, taken as a temperature at the midpoint of a baseline shift in heat flow characteristic of the transition.

TGA measurements were carried out with a TA Instruments TGA2950 apparatus in two different atmospheres: one is a nitrogen flow and the other is an air flow (dynamic air), both with a constant rate of 100 mL min^{-1}. Each measurement was made on ca. 10-mg of the sample (vacuum-dried at 40 °C in advance), which was heated from 25 to 700 °C at a scanning rate of 2 °C min^{-1}. The temperature of polymer degradation, T_d, was taken as a temperature at the onset point of the weight loss in the TGA curve obtained. All the measurements were duplicated and the response of the TGA traces was essentially reproducible; for example, the reproducibility of T_d data was within ±1 °C.

FT-IR spectra were recorded on a Shimadzu FT-IR8600PC apparatus by the ordinary KBr method at a sample concentration of 1 wt %, over a wavenumber range 400–2000 cm^{-1} with a resolution of 4 cm^{-1} via accumulation of 32 scans.

Results and discussion

NMR characterization of CPs

Propionyl DS and its distribution of CP1 and CP2 were estimated by NMR spectroscopy. After thorough acetylation (see Experimental section), the acetylated CPs were well soluble in $CDCl_3$, giving rise to well-resolved ^{1}H and ^{13}C NMR spectra. A ^{1}H spectrum of acetylated CP2 is illustrated in Fig. 1, together with resonance-peak assignments. In the spectrum, we designate a resonance peak area derived from the methyl protons of propionyl groups as **A**; a total resonance area both from the methyl protons of acetyl groups and from the methylene protons of propionyl groups as **B**; and an area derived from the seven protons of the anhydroglucose residue as **C**. Then the propionyl DS ($DS_{Pr\text{-}NMR}$) and acetyl DS (DS_{Ac}) can be determined by Eqs. (1) and (2), respectively.

$$DS_{Pr\text{-}NMR} = (\mathbf{A} / 3) / (\mathbf{C} / 7) \qquad (1)$$

$$DS_{Ac} = [(\mathbf{B} - 2\mathbf{A} / 3) / 3] / (\mathbf{C} / 7) \qquad (2)$$

<<**Figure 1**>>

The distribution of propionyl groups was analyzed by using an inverse-gated decoupling ^{13}C NMR technique. In Fig. 2, ^{13}C spectra of acetylated CP1 and CP2 are shown for a region of carbonyl signals, together with the peak assignments. To determine the measuring conditions (see Experimental section) and also to assign carbonyl carbons for acetyl and propionyl groups at the C2, C3, and C6 positions of cellulose, we referred to a study by Tezuka and Tsuchiya (1995). In the spectra, we designate a resonance peak area derived from the carbonyl carbon of the propionyl group at C2 as **D**, and similarly define **E** and **F** as

to the propionyl groups at C3 and C6, respectively. Then the propionyl DSs at C2, C3 and C6 in the anhydroglucose residue can be evaluated by Eqs. (3), (4), and (5), respectively.

$$DS_{Pr} \text{ at C2} = DS_{Pr\text{-}NMR} \times \mathbf{D} / (\mathbf{D} + \mathbf{E} + \mathbf{F}) \quad (3)$$

$$DS_{Pr} \text{ at C3} = DS_{Pr\text{-}NMR} \times \mathbf{E} / (\mathbf{D} + \mathbf{E} + \mathbf{F}) \quad (4)$$

$$DS_{Pr} \text{ at C6} = DS_{Pr\text{-}NMR} \times \mathbf{F} / (\mathbf{D} + \mathbf{E} + \mathbf{F}) \quad (5)$$

<<**Figure 2**>>

Table 1 summarizes a result of the determination of the propionyl distribution as well as that of the assessment of $DS_{Pr\text{-}NMR}$ and DS_{Ac} for acetylated CP1 and CP2. It turns out that the most important difference between the two CPs was in DS_{Pr} at C6. The primary OH group at C6 of CP1 was fully propionylated, while 20 % of C6 hydroxyls of CP2 was free and available for phosphorylation.

<<**Table 1**>>

Molecular weight of CPs

Molecular weights of the two acetylated CPs were evaluated by GPC. Table 2 compiles data of the number-average molecular weight (M_n), weight-average molecular weight (M_w), degree of polydispersity (M_w/M_n), and weight-average degree of polymerization (DP_w) of the derivatives. DP_w was estimated by division of M_w by a calculated molecular mass per

repeating unit of the respective acetylated CPs. From the result of the GPC analysis, it should be reasonable to assume that the molecular weights of the two CPs (non-acetylated) were comparable to each other.

<<**Table 2**>>

Characterization of phosphorylated CP derivatives

DS_{Pr} and phosphoryl DS (DS_{Ph}) values of phosphorylated CP derivatives were estimated by elemental analysis and a wet chemical quantification. The latter analysis is composed of a series of procedures of saponification and successive HPLC quantification of the resulting propionic acid production. DS_{Pr} values of the original CP1 and CP2 samples were also estimated by the wet chemical analysis to ensure the validity of the quantification with NMR. Table 3 summarizes data of C and P contents (from elemental analysis), propionyl side-chain content (Pr % in weight ; from wet chemical analysis), and DS_{Pr} and DS_{Ph} values, estimated for CP1, CP2, and their respective phosphorylated derivatives. The DS_{Pr} and DS_{Ph} were calculated by the following Eqs. (6) and (7), respectively.

$$DS_{Pr} = [Pr\ \% / FW_{Pr}] / [(100 - Pr\ \% - Phos\ \%) / FW_{AGU}] \quad (6)$$

$$DS_{Ph} = [Phos\ \% / FW_{Phos}] / [(100 - Pr\ \% - Phos\ \%) / FW_{AGU}] \quad (7)$$

where Phos % is a phosphoryl side-chain content (in weight) which was determined by using a P : C content ratio obtained from the elemental analysis, FW_{AGU} (= 162.14) and FW_{Pr} (= 56.06) are formula weights of AGU and propionyl unit, respectively, and FW_{Phos} is a formula

weight of each phosphoryl side-chain introduced (DEP = 136.09; DETP = 152.15; DMP = 108.03; DMTP = 124.10).

<<**Table 3**>>

As seen in Table 3, the DS_{Pr} values of the two CPs are found to be in good accordance with the corresponding data from NMR measurements (Table 1). After the phosphorylation, however, their DS_{Pr}s decreased to some extent. Particularly, the decrement was noticeable in the DEP and DETP derivatives of CP1, attended by a comparatively larger gain in DS_{Ph} (> 0.6); this can be attributed to transesterification as well as to depropionylation in the reaction process with the corresponding phosphoryl chlorides. As a result, the parameter DS_{Ph} for the CP1 derivative series varied widely depending on the chemical structure of the phosphoryl substituent. On the other hand, the CP2 derivatives showed a mutually close DS_{Ph} value. In connection with the present derivatization, there was a review noting a preferential substitution at the C6 site for a reaction between orthophosphoric acid and cellulose (Nehls et al. 1994). In view of these observations and TGA data shown below, it is inferred that the degree of C6-*O* phosphorylation for the CP2 derivatives is generally higher than that for the CP1 series, but the DEP-CP1 and DETP-CP1 products would have a certain quantity of phosphoryl groups at C6 via the sub-effect of transesterification despite the thorough propionyl-protection at the position. Although we attempted the regioselectivity estimation for the CP derivatives using NMR measurements, it was difficult because of their lower solubility as shown in the next paragraph.

Table 4 shows a result of a solubility test using different solvents (THF, $CHCl_3$, DMSO, DMF, and Py) for CP1, CP2, and their phosphorylated derivatives. The solubility was judged from the dissolution behaviour of 5 mg of each sample in 1 mL of the respective

solvents (20 °C). As a general trend, the phosphorylation/thiophosphorylation deteriorated the solubility of the starting CPs. The thiophosphorylated CP derivatives exhibited higher solubility in most of the solvents employed here, compared with the S-free, phosphorylated ones from the same CP. The exceptionally better solubility of DMP-CP1 is probably owing to the comparatively low DS_{Ph} (= 0.06). The solubility of DETP-CP2 was high, but it was still lower than that of the original CP2, judging from a little bit slower dissolution of the former sample.

<<**Table 4**>>

Thermal properties of cellulose, CPs, and phosphorylated CP derivatives

A comparative study of thermal properties was performed for cellulose (Avicel), CPs, and phosphorylated CP derivatives. First, we estimated T_g and $T_{d\text{-}DSC}$ of the samples by DSC. Figure 3 displays the thermograms obtained in the second heating scan. In the thermograms, up-pointing arrows indicate a $T_{d\text{-}DSC}$ position, and downward arrows represent a T_g position. (Note that the $T_{d\text{-}DSC}$ positions marked are in the first heating scan, and that the corresponding positions in the second scan are deviated from the respective first ones, but without large discrepancies (< 3 °C)). The T_g and $T_{d\text{-}DSC}$ data thus evaluated are listed in Table 5.

<<**Figure 3**>>

<<**Table 5**>>

Pure cellulose (Avicel) exhibited neither T_g nor $T_{d\text{-}DSC}$ up to 300 °C. CP1 and CP2

showed a clear baseline shift reflecting the glass transition in the thermograms and their T_gs were evaluated as 150.5 °C and 145.1 °C, respectively, but no thermal degradation signal appeared below 300 °C. Concerning the phosphorylated CP1 and CP2 series, any of the derivatives imparted a T_g (135–167 °C) and a baseline elevation signalizing the exothermic degradation. The onset point of the exothermic reaction, $T_{d\text{-}DSC}$, varied depending on the structure of the phosphoryl side-chain moiety. As an explicit tendency, $T_{d\text{-}DSC}$ values of thiophosphorylated samples (DETP-CPs and DMTP-CPs) were lower than those of the others having normal phosphoryl groups free of sulfur, and the comparatively bulky diethyl(thio)phosphorylated derivatives (DEP-CPs and DETP-CPs) began to degrade in an earlier stage of the heating, relative to the dimethyl(thio)phosphorylated ones.

The lowering in $T_{d\text{-}DSC}$ with the sulfur introduction may be interpreted as being primarily due to a possible structural transformation, such as that shown in Scheme 1 (Katsuura and Inagaki 1978), which preceded the actual degradation of the thiophosphorylated CP derivatives. A similar observation of T_d-depression has been experienced by Kaur et al. (1987) in a differential thermal analysis (DTA) for cellulose phosphate and cellulose thiophosphate; an apparent T_d as the starting temperature of exothermic ascent in the DTA was estimated as 228 °C for the phosphate and 220 °C for the thiophosphate. The research group also referred to the transformation reaction (I to II in Scheme 1), but they concluded that the pyrolysis itself of the cellulose thiophosphate occurred in a manner similar to that for the cellulose phosphate, i.e., the catalytic effect of thiophosphoric acid for char formation was substantially equivalent to that of ordinary phosphoric acid.

<<**Scheme 1**>>

Next we examined thermal degradation behaviour by TGA. Figure 4 compiles TGA

curves of Avicel, CP1, CP2, and phosphorylated derivatives of the CPs. The measurements were carried out in dynamic air as well as in a nitrogen flow. Data of T_d and residual weight at 700 °C (in percentage relative to the weight at 100 °C) are summarized in Table 5.

Under the N_2 atmosphere, all the samples exhibited a monomodal weight-loss curve (Figs. 4a, b, and c). The weight loss of Avicel and CPs started at around 300 °C, and that of the phosphorylated CP derivatives initiated roughly at 200–250 °C. Evidently, the phosphoryl groups promote the thermal degradation reaction of the cellulosic polymers (and therefore the heat resistance as a bulk material is lowered), but the char generation (and therefore the flame resistance) is markedly encouraged instead. Such a T_d drop accompanying the char promotion is well known empirically for cellulose materials containing a phosphoryl compound as flame retarder (e.g. Gottlieb 1956; Kandola et al. 1996). A relatively higher T_d observed for DMP-CP1 is owing mainly to the lower DS_{Ph}. When the data of weight residue at 700 °C are compared among the phosphorylated CP samples exposed to N_2 gas, the value is found to increase with increasing DS_{Ph} and therefore with increasing P content.

<<**Figure 4**>>

Under the air flow, Avicel, CP1, CP2, and the phosphorylated CP1 derivatives showed a bimodal weight loss curve (Figs. 4d and e), while the phosphorylated CP2 derivatives exhibited a basically monomodal weight loss curve (Fig. 4f). As a consequence of the difference of whether the second weight loss took place or not above 450 °C, the ultimate percentages of weight residue (9.7–15.7 %) for the CP2 derivatives were considerably higher than those (2.5–6.1 %) for the CP1-based samples. In Table 5, data of the onset point of the first weight loss are listed as T_d (air) estimated by TGA. The T_d (air) values, and also T_d (N_2)

ones estimated similarly in N_2, for all the phosphorylated CPs were in good accordance in the order of relative magnitude with the corresponding data determined by DSC. However, both of the T_ds obtained by TGA were habitually somewhat lower than $T_{d\text{-}DSC}$ in the S-free phosphorylated series, whereas there was a tendency of the reverse in the thiophosphorylated series. The latter observation is probably due to the structural transformation of the thiophosphoryl substituents, the reaction occurring right before the actual polymer pyrolysis.

IR study of char

Figure 5 displays FT-IR spectra of Avicel, CP1, CP2, and phosphorylated CP derivatives. Before the measurement, each sample was subjected to a heat treatment from 25 to 400 °C at a rate of 2 °C min^{-1} under dynamic air. The heating condition is identical to that of the TGA measurement in air, but the latter experiment was done up to 700 °C. Therefore, the FT-IR data should characterize an intermediate residue in the process of pyrolysis of the respective samples. The wavenumbers and assignments of observed and potentially detectable IR-bands are listed in Table 6 together with available references (Balabanovich et al. 2003; Bourbigot et al. 1995; Kandola and Horrocks 1996; Katsuura and Inagaki 1978; Kaur et al. 1987; Luneva and Oputina 1997; McKee et al. 1984; Singh et al. 1979; Suárez-García et al. 2002).

<<**Figure 5**>>

<<**Table 6**>>

As shown in Fig. 5a, IR spectra of the intermediate residues in pyrolysis of Avicel, CP1,

and CP2 were quite similar to each other. Formerly Jain et al. (1985) also reported that IR bands inherent in cellulose propionate disappeared completely after heat-treating from ambient temperature to 400 °C in an air flow. From these evidences, it can be taken that the resultant char at 400 °C of Avicel and those of the CP samples are essentially the same in chemical composition, even though the quantities of the residues are different from each other. In the IR data for these three samples, a peak at 1710 cm^{-1} (νC=O) and that at 1600 cm^{-1} (νC=C) are more prominent as twin signals, rather than the appearance of a broad peak centering ~1200 cm^{-1} which involves a ν_{as}C-O band of aliphatic char (1150 cm^{-1}) and a similar stretching band of aromatic char (1240 cm^{-1}).

With regard to the phosphorylated CP derivatives, the IR spectra (Figs. 5b–e) exhibit new bands at 500 cm^{-1} (δO-P-O; νP-S) and 1000 cm^{-1} (νP-O-(C)) derived from phosphoryl groups; however, as to DMP-CP1 of lower DS_{Ph}, these two bands are feeble. Furthermore, the twin peaks at 1710 and 1600 cm^{-1} become apparently suppressed, relative to the broad peak lying in a 1100–1300 cm^{-1} region where plural stretching bands associated with some phosphoric compounds concentrate (see Table 6) in addition to the bands of aliphatic and aromatic chars. The presence of P=S was virtually indiscernible for the 400 °C residues of the DETP and DMTP derivatives. A matter of supreme significance is the difference in an intensity ratio I_{1710}/I_{1600} of the twin peaks between the phosphorylated CP1 and CP2 series. In both the series, the νC=O intensity I_{1710} is inferior to the νC=C intensity I_{1600} in contrast with the situation for the original CPs and Avicel; nevertheless, the degeneration of the carbonyl signal observed for the CP2 series is still greater than that for the CP1 series, as can be discerned in Figs. 5c–e. This implies that the intermediate residues in pyrolysis of the CP2 derivatives having a higher degree of C6-*O* phosphorylation contain fewer carbonyl components, in comparison with the corresponding residues of the CP1 derivatives phosphorylated preferentially at the C2/C3 positions. In Fig. 5b, exceptionally, there is less

difference in the I_{1710}/I_{1600} ratio between the IR data for DEP-CP1 and DEP-CP2. Presumably, the DEP-CP1 sample had been phosphorylated not only at C2 and C3, but also at C6 to a moderate extent via the transesterification effect, as is commented in the previous section.

Discussion of phosphorylation effect on char formation

A pyrolysis mechanism of cellulose has been described in detail by Kandola et al. (Kandola et al. 1996; Kandola and Horrocks 1996; Price et al. 1997). According to their papers, cellulose materials undergo two stages of pyrolysis reactions when heated in air to ~700 °C. Critical reactions in the first stage are dehydration and desaturation involved in AGU, occurring at temperatures of <400 °C, and the second stage comprises transglycosylation, cross-linking, and other oxidizing reactions at higher temperatures (> 400 °C). CP also seems to follow basically the same reaction route as the above (Jain et al. 1985); then, the temperature range for deesterification of CP should be comparable to that for the dehydration of cellulose per se in the first stage of pyrolysis, just as rationalized by the data of TGA (Fig. 4d) and IR (Fig. 5a).

The dehydration of cellulose, and the deesterification of CP as well, occur at the C2 and/or C3 positions preferably than do at C6, paralleling a so-called Zaitsev rule (Scotney 1972). A double bond resulting between C2 and C3 can transform into a C=O structure by a keto-enol tautomerism (discussed below). The remaining C6 hydroxyl group of cellulose attacks a $\beta(1\rightarrow4)$ glycosidic linkage, and the intermediate levoglucosan (or levoglucosenone) is formed and subsequently decomposes into volatile flammable compounds (Dobele et al. 1999). The C6-*O* propionyl group of CP would suppress, more or less, the formation of levoglucosan; however, the alkylester group decomposes completely and volatilizes before

the atmospheric temperature reaches 400 °C (Jain et al. 1985). The difference in T_d between CP1 and CP2, observed in the TGA study (see Table 5), may be partly derived from the difference in degree of the C6-*O* propionyl substitution between them.

If a phosphoric acid is present in the pyrolysis of cellulose materials, it acts as a catalyst to promote the dehydration and desaturation at temperatures much lower than 400 °C, usually enhancing the char content including nonvolatile phosphorous compounds. In the case, the desaturation of pyranose ring is achieved by two steps, hydroxyl phosphorylation and dephosphorylation. Therefore, if the cellulose is phosphorylated in advance, this dephosphorylation is equivalent to the sequential dehydration and desaturation reactions. A point to be emphasized in the present work is that the phosphoryl substituents introduced into the CP1 derivatives initiate the sequential reactions mainly at C2/C3 positions, while the corresponding moieties in the CP2 derivatives can expedite the reactions at C6 considerably. In order to clarify the difference in the earlier reaction stage of pyrolysis between the phosphorylated CP1 and CP2 derivatives, a scheme is shown in Fig. 6. The scheme was constructed by rearranging a part of the pyrolysis mechanism proposed for flame-retarded cellulose by Kandola and Horrocks (1996).

<<**Figure 6**>>

The CP1 derivatives phosphorylated largely at C2/C3 go through a reaction route designated **A** in Fig. 6. By heating the phosphoryl groups are easily eliminated below 400 °C and a double bond is formed between C2 and C3 in the glucopyranose ring. This C=C bond can actually equilibrate with a C=O structure by the keto-enol tautomerism. On the other hand, the CP2 derivatives phosphorylated preferentially at C6 are desaturated between C5 and C6 by dephosphorylation, as indicated as route **B** in Fig. 6. In this route, the

generation of carbonyl groups is inhibited.

After undergoing the respective main routes in the first stage of pyrolysis, both of the two series of CP derivatives deposit, temporarily, a certain amount of intermediates comprising carbonic residues and phosphoric compounds. For instance, at 300–400 °C, the weight amount depends predominantly on the total DS_{Ph} or P content of the sample concerned, as can be seen from mutual comparison of the TGA data in Figs. 4e and f; namely, DEP-CP1 and DETP-CP1, relatively rich in P content, exceed the corresponding CP2 derivatives in the weight residue at 400 °C.

In the second stage at temperatures of ca. 450–700 °C, there appears a remarkable contrast in the weight loss behaviour between the two phosphorylated CP series, again as we can see that regarding the TGA curves given in Figs. 4e and f. In the case of the CP1 derivatives, the carbonyl groups formed in the first stage can participate in a variety of fragmentation reactions leading to volatile acids, carbon monoxide and dioxide, etc. (Kandola et al. 1996), and hence they impart a comparatively steep drop in weight residue above 450 °C accompanied by the vigorous volatilization. The CP2 derivatives, on the contrary, possess fewer carbonyl groups after passing through the first stage of pyrolysis, as is really evidenced by the FT-IR data for the intermediate residues at 400 °C. Therefore, the derivatives show a rather gradual decrease in weight loss at temperatures higher than 450 °C, without undergoing such serious volatilization. This results in the observation of a higher yield of total chars nonflammable in air at 700 °C (see Table 5).

Conclusions

Two CPs were modified, respectively, into four derivative forms with various phosphoryl groups. A major difference between the starting CPs was whether the primary hydroxyl

group at C6 had been fully propionylated (CP1) or not (CP2), which was distinguished by an inverse-gated decoupling ^{13}C NMR technique. Propionyl DS (DS_{Pr}) and phosphoryl DS (DS_{Ph}) of the phosphorylated CP derivatives were successfully evaluated by elemental analysis and an additional method of saponification/HPLC coupling.

Thermal properties of cellulose (Avicel), CP1, CP2, and phosphorylated derivatives of the CPs were investigated by DSC and TGA measurements. The DSC analysis revealed that, as for the phosphorylated CP derivatives, the degradation-initiating temperature $T_{d\text{-}DSC}$ was invariably lowered relative to that for the corresponding original CP samples, but still sufficiently higher than the glass transition temperature T_g. In this respect, the phosphorylated CPs can be regarded as a tractable thermoplastic material. Especially thiophosphorylated CPs started the degradation at temperatures somewhat lower than those for the corresponding CPs normally phosphorylated, due to a possible structural transformation of the thiophosphoryl moiety, but those sulfur-containing derivatives showed better solubility in conventional organic solvents.

Estimation of thermal degradation behaviour by TGA was made both in N_2 and in air under a constant condition of flow. In the N_2 atmosphere, all of Avicel, CPs, and phosphorylated CPs exhibited a monomodal weight loss curve, and, at 700 °C, the CP derivatives provided a comparatively higher value of weight residue increasing with their DS_{Ph}. Under dynamic air, the cellulose, CPs, and phosphorylated CP1 derivatives showed a bimodal weight loss curve and their weight residues at 700 °C were very low (~6 wt % even for a CP1 derivative of higher DS_{Ph}). However, the CP2 derivatives gave a substantially monomodal loss curve and their weight residues at 700 °C were much higher (ca. 10–16 wt %).

The observed difference in thermal degradation (in air) between the two phosphorylated series was interpreted as due to the difference in selectivity of the preferential reaction route

of pyrolysis between them. The CP1 and CP2 derivatives are desaturated mainly at C2/C3 and at C6, respectively, following the dephosphorylation, and therefore the CP1 series is superior to the CP2 series in tautomeric formation of carbonyl groups that can participate in production of various flammable volatiles. This view was supported by the FT-IR measurements for the intermediate residues of pyrolysis of the phosphorylated samples.

From a practical standpoint, for example, the cellulose derivatives phosphorylated at C6 and propionylated at C2 and C3 may be taken as a multi-functional cellulosic material designed by using a regioselective modification technique. They excel in flame-resistance and processibility and have a potential for further developing as a flame-retardant for other polymers; namely, the blending or coating will be effective in protecting other combustible polymers against a rapid flame propagation. As a matter of fact, we carried out the UL94 vertical ignition test for some phosphorylated CP2 derivatives blended with poly(L-lactic acid) or poly(ethylene terephthalate) (Harada et al. 2010; Yamanaka et al. 2010). In consequence, the blend samples were judged to be a V-2 class incombustible material, supporting the above suggestion of utility. We are convinced that further optimization of side-chains of cellulose derivatives would expand their application range as thermoplastic flame resistant/retardant materials.

Acknowledgments This work was partially financed by a Grant-in-Aid for Scientific Research (A) (No. 20248019 to YN) from the Japan Society for the Promotion of Science.

References

Balabanovich AI, Balabanovich AM, Engelmann J (2003) Intumescence in poly(butylene terephthalate): the effect of 2-methyl-1,2-oxaphospholan-5-one 2-oxide and ammonium

polyphosphate. Polymer Int 52:1309–1314

Bourbigot S, Le Bras M, Delobel R, Bréant P, Trémillon JM (1995) Carbonization mechanisms resulting from intumescence – part II. Association with an ethylene terpolymer and the ammonium polyphosphoate-pentaerythritol fire retardant system. Carbon 33:283–294

Dobele G, Rossinskaja G, Telysheva G, Meier D, Faix O (1999) Cellulose dehydration and depolymerization reactions during pyrolysis in the presence of phosphoric acid. J Anal Appl Pyrolysis 49:307–317

El Seoud OA, Heinze T (2005) Organic esters of cellulose: new perspectives for old polymers. Adv Polym Sci 186:103–149

Gottlieb IM (1956) A theory of flame-retardant finishes. Text Res J 26:156–167

Harada T, Yamanaka Y, Yaginuma H, Nishio Y, Aoki D (2010b) Japan Patent, JP2010-31230A

Jain RK, Lal K, Bhatnagar HL (1985) Thermal, morphological, X-ray and spectroscopic studies on cellulose and its esters. J Anal Appl Pyrolysis 8:359–389

Kandola BK, Horrocks AR (1996) Complex char formation in flame-retarded fibre-intumescent combinations—II. Thermal analytical studies. Polymer Degrad Stab 54:289–303

Kandola BK, Horrocks AR, Price D, Coleman GV (1996) Flame-retardant treatments of cellulose and their influence on the mechanism of cellulose pyrolysis. J M S —Rev Macromol Chem Phys C36:721–794

Karakawa M, Takano T, Nakatsubo F (2007) Copolymerization of α-D-glucopyranose 1,2,4-ortho pivalate derivatives. Preparation of *O*-methyl celluloses with heterogeneous distribution of the methyl groups and their water solubility. Cellulose Chem Technol 41:555–561

Katsuura K, Inagaki N (1978) Flame-retardant properties of cellulose

phenylthiophosphonate. J Appl Polym Sci 22:679–687

Kaur B, Gur IS, Bhatnagar HL (1987) Thermal degradation studies of cellulose phosphates and cellulose thiophosphates. Angew Makromol Chem 147:157–183

Klemm D, Heublein B, Fink HP, Bohn A (2005) Cellulose: fascinating biopolymer and sustainable raw material. Angew Chem Int Ed 44:3358–3393

Luneva NK, Oputina AG (1997) Synthesis and properties of new esters of cellulose and inorganic polyacids containing phosphorus, molybdenum, tungsten and vanadium. Polym Eng Sci 37:940–944

McKee DW, Spiro CL, Lamby EJ (1984) The inhibition of graphite oxidation by phosphorus additives. Carbon 22, 285–290

Nehls I, Wagenknecht W, Philipp B, Stscherbina D (1994) Characterization of cellulose and cellulose derivatives in solution by high resolution ^{13}C-NMR spectroscopy. Prog Polym Sci 19:29–78

Nishio Y (2006) Material functionalization of cellulose and related polysaccharides via diverse microcompositions. Adv Polym Sci 205:97–151

Nishio Y, Matsuda K, Miyashita Y, Kimura N, Suzuki H (1997) Blends of poly(ε-caprolactone) with cellulose alkyl esters: effect of the alkyl side-chain length and degree of substitution on miscibility. Cellulose 4:131–145

Nishio Y, Roy SK, Manley RStJ (1987) Blends of cellulose with polyacrylonitrile prepared from *N*,*N*-dimethylacetamide—lithium chloride solutions. Polymer 28:1385–1390

Pacsu E, Schwenker RF Jr (1957) The effect of chemical modification on the flame and glow resistance of cotton cellulose. Text Res J 27:173–175

Price D, Horrocks AR, Akalin M, Faroq AA (1997) Influence of flame retardants on the mechanism of pyrolysis of cotton (cellulose) fabrics in air. J Anal Appl Pyrolysis 40–41:511–524

Scotney A (1972) The thermal degradation of cellulose triacetate—I The reaction products. Euro Polymer J 8:163–174

Singh BP, Srivastava G, Mehrotra RC (1979) Synthesis and reactions of triorganotin dialkyldithiophosphates. J Organometal Chem 171:35–41

Suárez-García F, Martínez-Alonso A, Tascón JMD (2002) A comparative study of the thermal decomposition of apple pulp in the absence and presence of phosphoric acid. Polymer Degrad Stab 75:375–383

Tezuka Y, Tsuchiya Y (1995) Determination of substituent distribution in cellulose acetate by means of a ^{13}C NMR study on its propanoated derivative. Carbohydr Res 273:83–91

Yamanaka Y, Harada T, Yaginuma H, Nishio Y, Aoki D (2010a) Japan Patent, JP2010-31229A

Figure Captions

Fig. 1 ^{1}H NMR spectrum and peak assignments of acetylated CP2 in $CDCl_3$

Fig. 2 ^{13}C NMR carbonyl region spectra of acetylated CP samples in $CDCl_3$, measured by an inverse-gated decoupling technique

Fig. 3 DSC thermograms of Avicel, CP1, CP2, and phosphorylated CP derivatives (second heating). Downward arrows indicate a T_g position taken as the midpoint of the discontinuity in heat flow in the second heating scan, and up-pointing arrows denote a $T_{d\text{-}DSC}$ position taken as the exothermic onset temperature in the first heating scan

Fig. 4 TGA curves of Avicel, CP1, CP2, and phosphorylated CP derivatives of the CPs, obtained in a gas flow of N_2 (a, b, and c) or air (d, e, and f). Data in (a) and (d): ——, Avicel; ·····, CP1; − − −, CP2. Data in (b) and (e): ——, DEP-CP1; ·····, DETP-CP1; − − −, DMP-CP1; −·−, DMTP-CP1. Data in (c) and (f): ——, DEP-CP2; ·····, DETP-CP2, − − −, DMP-CP2; −·−, DMTP-CP2

Fig. 5 FT-IR spectra of Avicel, CP1, CP2, and phosphorylated CP derivatives, measured after the samples were all heat treated from 25 to 400 °C at a rate of 2 °C min^{-1} under dynamic air. (a) Avicel, CP1, and CP2; (b) DEP-CP1 and DEP-CP2; (c) DETP-CP1 and DETP-CP2; (d) DMP-CP1 and DMP-CP2; (e) DMTP-CP1 and DMTP-CP2

Fig. 6 Scheme showing the reaction routes of pyrolysis of phosphorylated CP1 and CP2 derivatives, drawn up by partly rearranging a pyrolysis mechanism for flame-retarded

cellulose (Kandola and Horrocks 1996)

Scheme 1 Transformation of a thiophosphoryl group (Katsuura and Inagaki 1978)

In addition to the six figures and a scheme, there are six tables. See annexed sheets.

Table 1 DS values of acetylated CP1 and CP2, evaluated by ^{1}H and ^{13}C NMR

Samples	DS_{Pr} at C2	DS_{Pr} at C3	DS_{Pr} at C6	$DS_{Pr\text{-}NMR}$	DS_{Ac}
CP1	0.69	0.80	0.98	2.47	0.52
CP2	0.81	0.91	0.80	2.52	0.48

Table 2 M_n, M_w, M_w/M_n, and DP_w of acetylated CP1 and CP2, estimated by GPC

Samples	$M_n/10^4$	$M_w/10^4$	M_w/M_n	DP_w
CP1	6.01	16.92	2.82	525
CP2	8.04	18.82	2.34	582

Table 3 Data of C and P contents (from elemental analysis), propionyl content (from saponification and HPLC quantification), and DS_{Pr} and DS_{Ph} values for CP1, CP2 and their respective phosphorylated derivatives

Samples	C/wt %	P/wt %	Propionyl content/wt %	DS_{Pr}	DS_{Ph}
CP1	-	-	45.60	2.42	-
DEP-CP1	44.60	7.49	25.91	1.83	0.96
DETP-CP1	44.60	5.71	27.98	1.81	0.65
DMP-CP1	52.15	0.63	41.83	2.16	0.06
DMTP-CP1	46.74	3.74	36.57	2.19	0.39
CP2	-	-	45.78	2.44	-
DEP-CP2	48.70	4.11	36.66	2.35	0.48
DETP-CP2	48.73	2.91	36.91	2.17	0.30
DMP-CP2	49.75	3.24	36.30	2.01	0.33
DMTP-CP2	48.31	3.32	34.62	1.91	0.32

Table 4 Solubility of CP1, CP2, and phosphorylated CP derivatives in various solvents

Samples	THF	$CHCl_3$	DMSO	DMF	Py
CP1	+	+	+	+	+
DEP-CP1	−	−	(+)	(+)	(+)
DETP-CP1	+	−	+	+	+
DMP-CP1	+	(+)	+	+	+
DMTP-CP1	+	(+)	+	+	+
CP2	+	+	+	+	+
DEP-CP2	−	−	(+)	(+)	(+)
DETP-CP2	+	+	+	+	+
DMP-CP2	(+)	−	(+)	(+)	(+)
DMTP-CP2	(+)	−	+	+	+

+, Soluble; (+), Swollen; −, Insoluble.

Table 5 Values of T_g, T_d, and weight residue at 700 °C for cellulose (Avicel), CP1, CP2, and phosphorylated CP derivatives, estimated by DSC and TGA

Samples		T_g /°C	$T_{d\text{-}DSC}$ /°C	T_d (N_2) /°C	T_d (air) /°C	Weight Residue at 700 °C/wt %	
Code	P content/wt %					in N_2	in air
Avicel	-	n.d.	n.d.	304.9	282.0	5.0	0.6
CP1	-	150.5	n.d.	318.8	304.6	10.0	0.9
CP2	-	145.1	n.d.	307.6	281.9	12.0	0.7
DEP-CP1	7.49	150.2	205.9	198.9	198.3	29.7	6.1
DETP-CP1	5.71	138.1	181.7	194.0	195.5	27.5	2.5
DMP-CP1	0.63	149.0	250.0	246.4	241.9	18.9	4.2
DMTP-CP1	3.74	151.4	189.4	200.4	199.6	26.6	4.1
DEP-CP2	4.11	135.3	218.7	208.1	212.9	24.6	9.7
DETP-CP2	2.91	139.2	210.3	201.6	202.2	24.7	14.9
DMP-CP2	3.24	151.6	237.8	237.6	235.5	23.6	15.5
DMTP-CP2	3.32	167.4	224.1	230.5	234.1	27.0	15.7

n.d.: could not be detected.

Table 6 Band assignments for infrared spectra (Fig. 5) of the residues at 400 °C of heat-treated Avicel, CPs, and phosphorylated CP derivatives

Wavenumber/ cm^{-1}	Assignment	References
500	δO-P-O	(Luneva and Oputina 1997; McKee et al. 1984)
	νP-S	(Katsuura and Inagaki 1978; Singh et al. 1979)
710	νP=S	(Katsuura and Inagaki 1978; Singh et al. 1979)
900	ν_{as}P-O in P-O-P	(Balabanovich et al. 2003; Kaur et al. 1987; Luneva and Oputina 1997; Bourbigot et al. 1995)
1000	νP-O-(C)	(Balabanovich et al. 2003; Singh et al. 1979)
1050	νO-P	(McKee et al. 1984)
1100	ν_{s}P-O in P-O-P	(Bourbigot et al. 1995)
1150	ν_{as}C-O in aliphatic compound	(Suárez-García et al. 2002)
	νC-O-(P)	(Singh et al. 1979)
	ν_{as}C-O-C bridge stretching of pyranose ring	(Kandola and Horrocks 1996; Kaur et al. 1987; Suárez-García et al. 2002)
1200	νP-O-(C) of phosphate-carbon ester complexes	(Bourbigot et al. 1995; McKee et al. 1984; Suárez-García et al. 2002)
1240	ν_{as}C-O of aromatic compound	(Suárez-García et al. 2002)
	νP=O	(Balabanovich et al. 2003; Katsuura and Inagaki

		1978; Kaur et al. 1987; Luneva and Oputina 1997)
1440	δ_{as}C-H	(McKee et al. 1984; Suárez-García et al. 2002)
1600	νC=C	(Katsuura and Inagaki 1978; Kaur et al. 1987; McKee et al. 1984; Suárez-García et al. 2002)
1710	νC=O	(Balabanovich et al. 2003; Katsuura and Inagaki 1978; Kaur et al. 1987; Suárez-García et al. 2002)

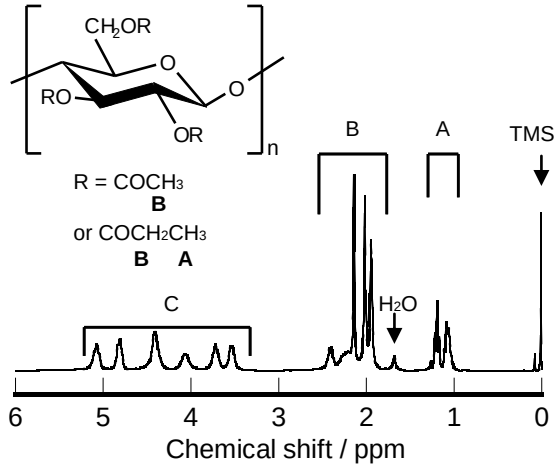

Fig. 1 ^{1}H NMR spectrum and peak assignments of acetylated CP2 in $CDCl_3$

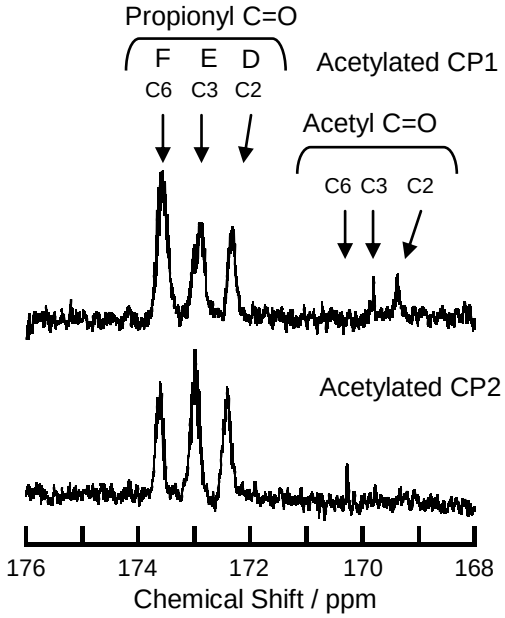

Fig. 2 ^{13}C NMR carbonyl region spectra of acetylated CP samples in $CDCl_3$, measured by an inverse-gated decoupling technique

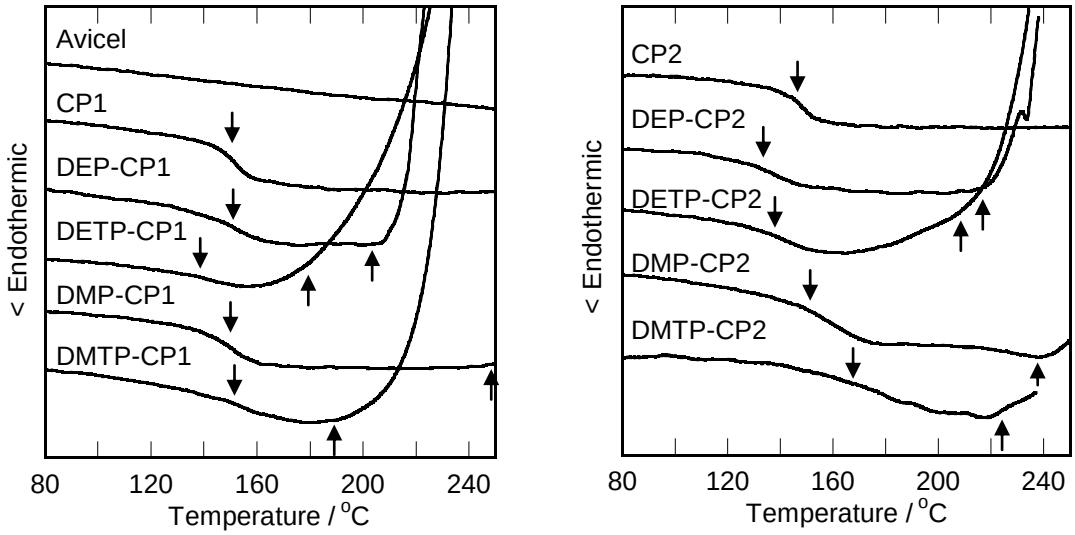

Fig. 3 DSC thermograms of Avicel, CP1, CP2, and phosphorylated CP derivatives (second heating). Downward arrows indicate a T_g position taken as the midpoint of the discontinuity in heat flow in the second heating scan, and up-pointing arrows denote a $T_{d\text{-}DSC}$ position taken as the exothermic onset temperature in the first heating scan

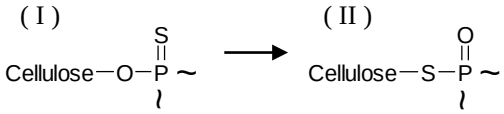

Scheme 1 Transformation of a thiophosphoryl group (Katsuura and Inagaki 1978)

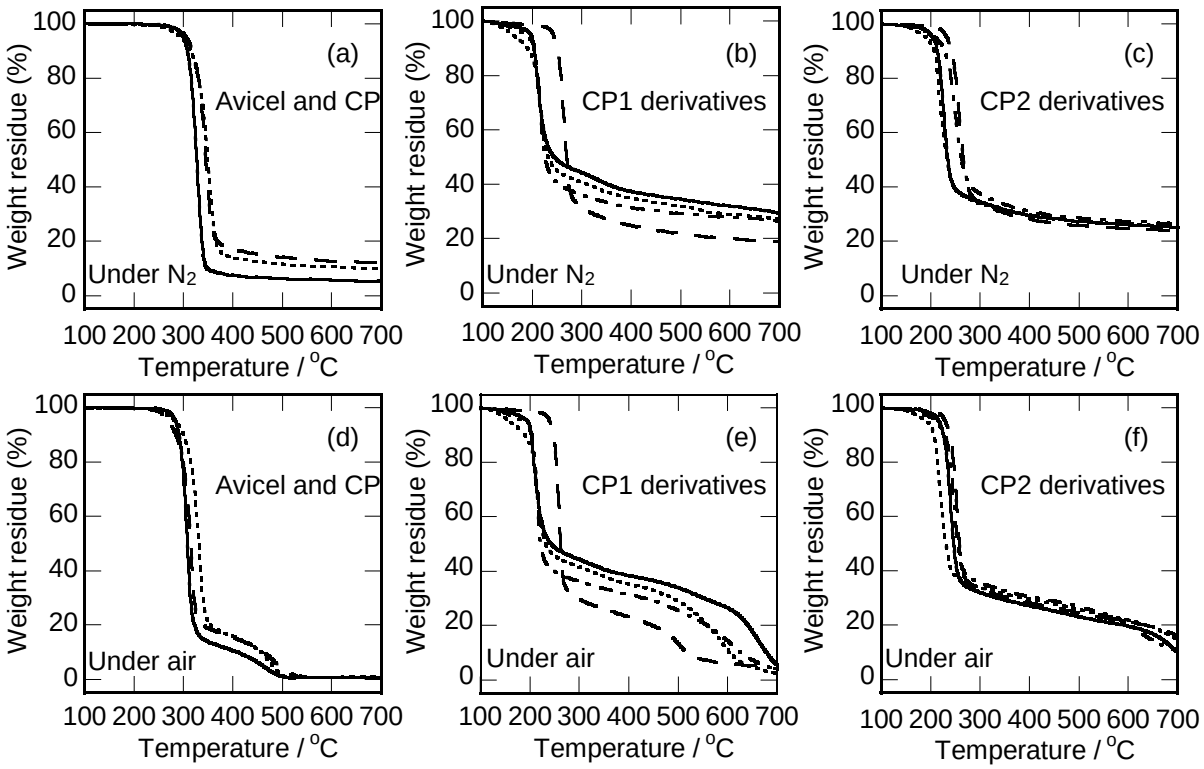

Fig. 4 TGA curves of Avicel, CP1, CP2, and phosphorylated CP derivatives of the CPs, obtained in a gas flow of N_2 (a, b, and c) or air (d, e, and f). Data in (a) and (d): ——, Avicel; ·····, CP1; − − −, CP2. Data in (b) and (e): ——, DEP-CP1; ·····, DETP-CP1; − − −, DMP-CP1; −·−, DMTP-CP1. Data in (c) and (f): ——, DEP-CP2; ·····, DETP-CP2, − − −, DMP-CP2; −·−, DMTP-CP2

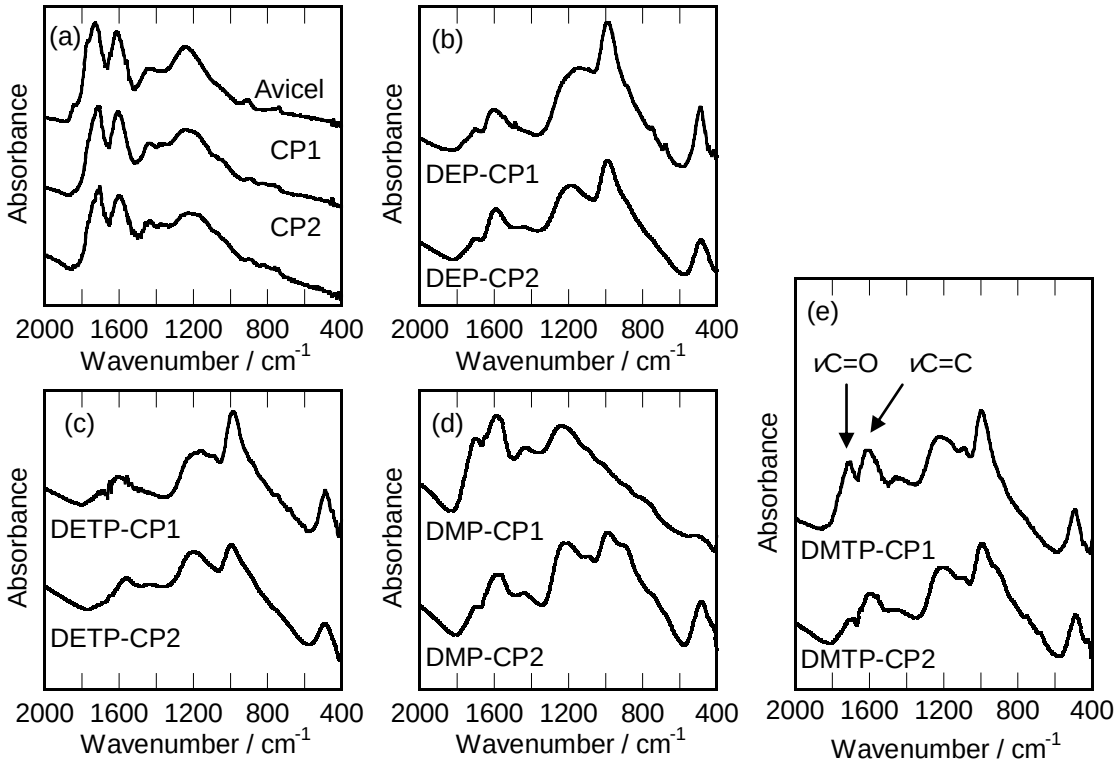

Fig. 5 FT-IR spectra of Avicel, CP1, CP2, and phosphorylated CP derivatives, measured after the samples were all heat treated from 25 to 400 °C at a rate of 2 °C min^{-1} under dynamic air. (a) Avicel, CP1, and CP2; (b) DEP-CP1 and DEP-CP2; (c) DETP-CP1 and DETP-CP2; (d) DMP-CP1 and DMP-CP2; (e) DMTP-CP1 and DMTP-CP2

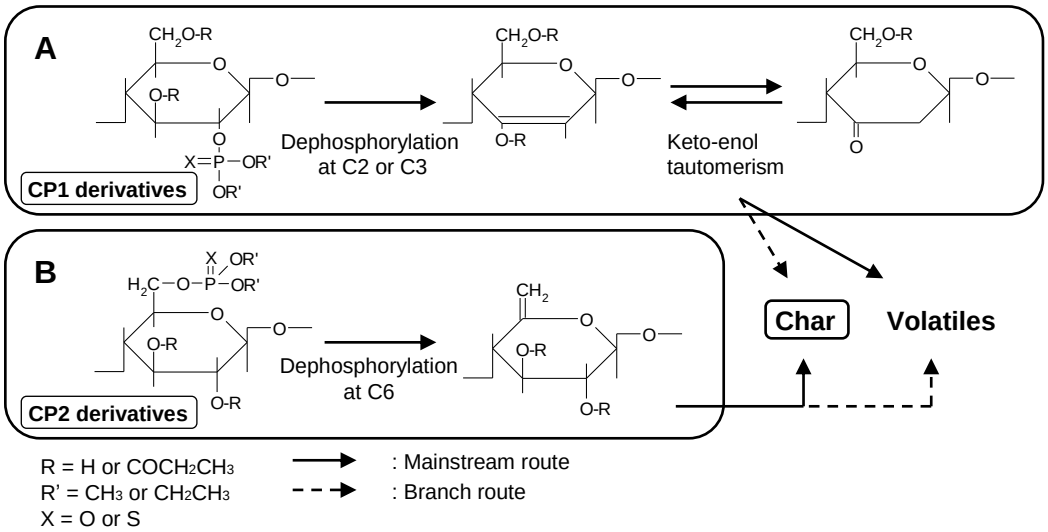

Fig. 6 Scheme showing the reaction routes of pyrolysis of phosphorylated CP1 and CP2 derivatives, drawn up by partly rearranging a pyrolysis mechanism for flame-retarded cellulose (Kandola and Horrocks 1996)